ELSEVIER

Journal of Alloys and Compounds 300–301 (2000) 152–157

Journal of ALLOYS AND COMPOUNDS

www.elsevier.com/locate/jallcom

Investigation of $LiXO_3$ (X=Nb, Ta) crystals doped with luminescent ions Recent results

W. Ryba-Romanowski*, I. Sokólska, G. Dominiak-Dzik, S. Gołąb

Institute of Low Temperature and Structure Research, Polish Academy of Sciences, Wrocław, Poland

Abstract

Processes of transfer of excitation from levels populated by diode laser pumping to upper laser levels in $LiTaO_3$:Tm and $LiTaO_3$:Ho are considered. Stimulated emission cross section for the $^3F_4-^4H_6$ transition of Tm and for the $^5I_7-^5I_8$ transition of Ho in lithium tantalate have been evaluated. Preliminary data concerning the contribution of radiative transitions and multiphonon relaxation to the decay of excited states of Er, Tm and Ho in $LiNbO_3$ and $LiTaO_3$ are compared.

Keywords: Luminescent ions; Stimulated emission cross section; Radiative transitions

1. Introduction

Single crystals of $LiNbO_3$ and $LiTaO_3$ have been studied intensively during several decades and their properties are well documented in numerous original works and review papers [1–3]. Owing to advantageous electrooptic, acoustooptic and nonlinear optical characteristics these materials found wide application in optoelectronic devices.

When doped with rare earth ions, the $LiNbO_3$ and $LiTaO_3$ crystals become luminescent media able to generate and amplify light. This ability, combined with inherent nonlinear properties, offers a possibility to design self Q switching and self frequency doubling laser sources.

Laser action in $LiNbO_3$ doped with Nd, Tm and Ho were obtained 30 years ago [4] but subsequent studies focused on Nd doped crystals [5,6]. Recently, interest in these systems has been renewed because of spectacular progress in the field of semiconductor laser which became convenient sources for the design of all integrated solid state lasers. In a number of recent papers the performance of laser diode pumped $LiNbO_3$:Nd and $LiTaO_3$:Nd lasers has been examined [7,8]. Also, the light generation and amplification in $LiNbO_3$:Er crystal has been considered aiming at its application in telecommunication systems [9]. Considerable effort has been done to understand the nature and number of activator sites in $LiNbO_3$ [10–14], but this problem is still open in the case of $LiTaO_3$. Little is known about the excitation and decay of activators in both the compounds doped with rare earth ions. Moreover, scarce published data are frequently inconsistent. The intention of this work is to get a closer insight into processes contributing to the relaxation of excited states and to assess the laser potential of selected rare earth ions in $LiNbO_3$ and $LiTaO_3$.

2. Crystal structure and selected physicochemical properties of $LiNbO_3$ and $LiTaO_3$

Properties of undoped lithium niobate and lithium tantalate may be found in numerous handbooks. Therefore we recall in Table 1 these data which are relevant to optical characteristics of doped systems. $LiNbO_3$ and $LiTaO_3$ are isostructural with nearly the same lattice

Table 1
Crystal structure and selected physicochemical properties of $LiNbO_3$ and $LiTaO_3$[a]

Compound	$LiNbO_3$	$LiTaO_3$
Space group	*R3c*	*R3c*
Lattice constants	$a=5.15$ Å	$a=5.14$ Å
	$c=13.86$ Å	$c=13.74$ Å
Density [g/cm^3]	4.64	7.45
Melting point [°C]	1210	1650
Index of refraction	$n_o=2.278$	$n_o=2.175$
	$n_e=2.195$	$n_e=2.180$
	($\lambda=0.667$ μm)	($\lambda=0.7$ μm)
Birefringence	−0.0825	+0.005

[a] Congruent composition: Li/Nb(Ta)=0.94.

*Corresponding author.
E-mail address: intibs@int.pan.wroc.pl (W. Ryba-Romanowski)

0925-8388/00/$ – see front matter
PII: S0925-8388(99)00715-X

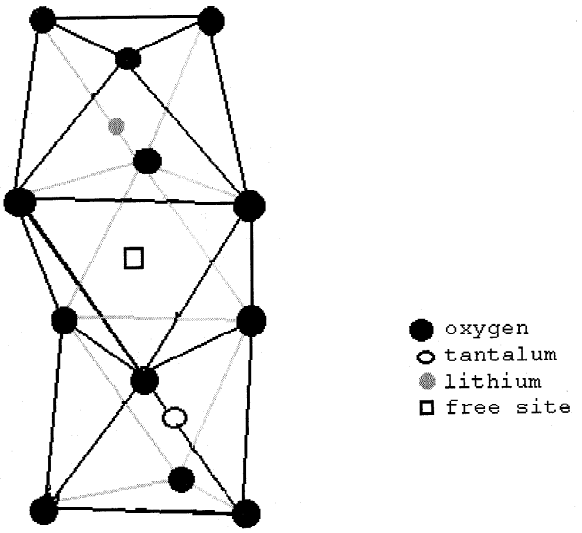

Fig. 1. The crystal structure of $LiTaO_3$.

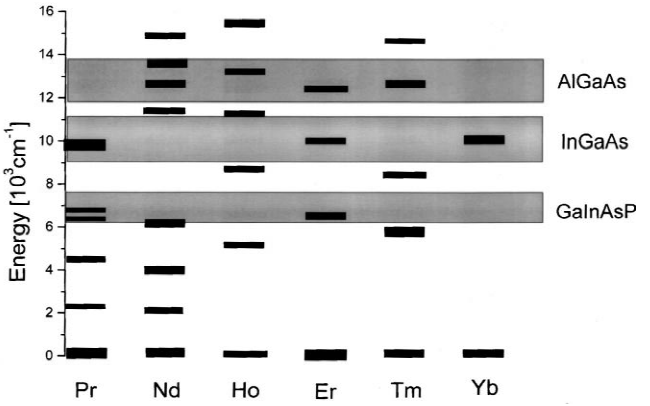

Fig. 2. Low lying energy levels of selected rare earth ions together with spectral emission of available powerful laser diodes.

parameters, but the density of the later compound is considerably higher. Melting point of $LiTaO_3$ is such that iridium crucibles are necessary to grow the crystals and consequently this material is more expensive as compared to $LiNbO_3$. Birefringence of $LiNbO_3$ is sufficiently high to allow phase matching in SHG process, but the relation between birefringence and dispersion of $LiTaO_3$ is less favorable and the quasi phase-matching method should be used.

Considering the structural impact on rare earth ions in doped crystals, one should remember that the chemical composition of $LiNbO_3$ and $LiTaO_3$ is not stoichiometric but corresponds to congruent melt with Li/Nb (Ta) ratio of about 0.94. Consequently, lithium deficiency gives rise to certain structural disorder resulting in inhomogeneous broadening of spectral lines associated with electronic transitions of rare earth ions. Ideal structure of stoichiometric compound shown in Fig. 1 indicates that three similar sites may be occupied by rare earth ions, namely Nb^{5+} site, Li^+ site and a free site. In all these sites rare earth ions reside in distorted octahedra of oxygen ions and have identical symmetry dose to C_3. In compounds with congruent composition a disorder resulting from a need of charge compensation is accompanied by a disorder associated with Li deficiency.

Consequently, several non-equivalent sites of rare earth ions in $LiNbO_3$ and $LiTaO_3$ may be identified based on spectroscopic data [10–12].

3. Laser transitions of primary interest

Considering laser transitions in rare earth doped $LiNbO_3$ and $LiTaO_3$ availability of pump source, pumping efficiency and processes leading to the population build-up on upper laser level should be accounted for. In Fig. 2, low-lying energy levels of selected rare earth ions are indicated together with spectral regions of emission of available powerful laser diodes. It can be seen that the emission bands of these pump sources coincide quite well with energy levels of rare earth ions. Suitability of laser diodes for optical pumping of $LiNbO_3$:Nd, $LiTaO_3$:Nd and $LiNbO_3$:Er lasers has been demonstrated, therefore in following we will restrict our consideration to holmium and thulium doped crystals, which seem to be the most promising systems. In Fig. 3 the partial energy level scheme for $LiTaO_3$:Tm is shown. Emission wavelength of an AlGaAs laser diode matches perfectly an absorption band associated with the $^3H_6$–$^3H_4$ transition whose intensity is sufficiently high to ensure efficient pumping. By a cascade relaxation through the $^3H_5$ level, the $^3F_4$ level is populated, which in turn decay by radiative transition to the ground $^3H_6$ level. One of the most important parameters which determine the laser performance of an active material is a stimulated emission cross section. In the most simple approach it can be evaluated by the so-called reciprocity method which relies on the absorption cross section and emission cross section according to the formula:

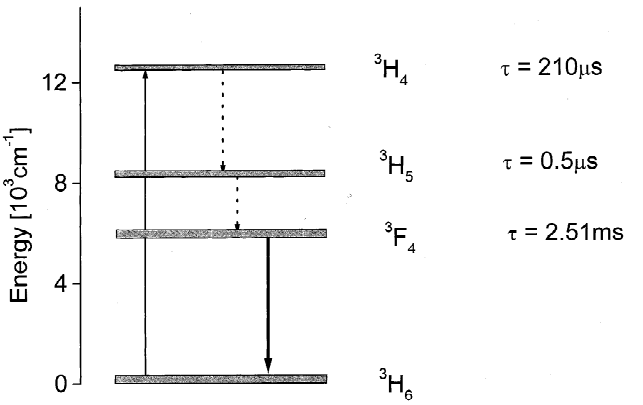

Fig. 3. The partial energy level scheme for Tm^{3+} in $LiTaO_3$.

$$\sigma_{em}(\lambda) = \sigma_{abs}(\lambda)\frac{Z_l}{Z_u}\exp\left[\frac{\left(E_{ul} - \frac{hc}{\lambda}\right)}{kT}\right] \quad (1)$$

where $\sigma_{abs}(\lambda)$ is absorption cross-section defined as $\sigma_{abs} = \alpha/N$, α is the absorption coefficient calculated from room temperature spectrum, N is the dopant concentration, E_{ul} is zero-line energy for interacting manifolds and Z_l, Z_u are the partition functions of the lower and upper manifolds, respectively.

To make use of this formula the room temperature absorption spectrum and energies of the crystal field levels of an upper and lower multiplets are needed. Having the crystal field levels located from low temperature absorption and emission spectra, the stimulated emission cross section has been derived for π and σ polarization. Results for $LiTaO_3$:Tm are shown in Fig. 4. The curves of potential laser gain versus wavelength will be red shifted because of a self-absorption. They can be calculated as the effective cross sections σ_{eff} according to the formula:

$$\sigma_{eff} = P\sigma_{em} - (1-P)\sigma_{abs} \quad (2)$$

where P is defined as a number of active ions in excited state to total number of active ions.

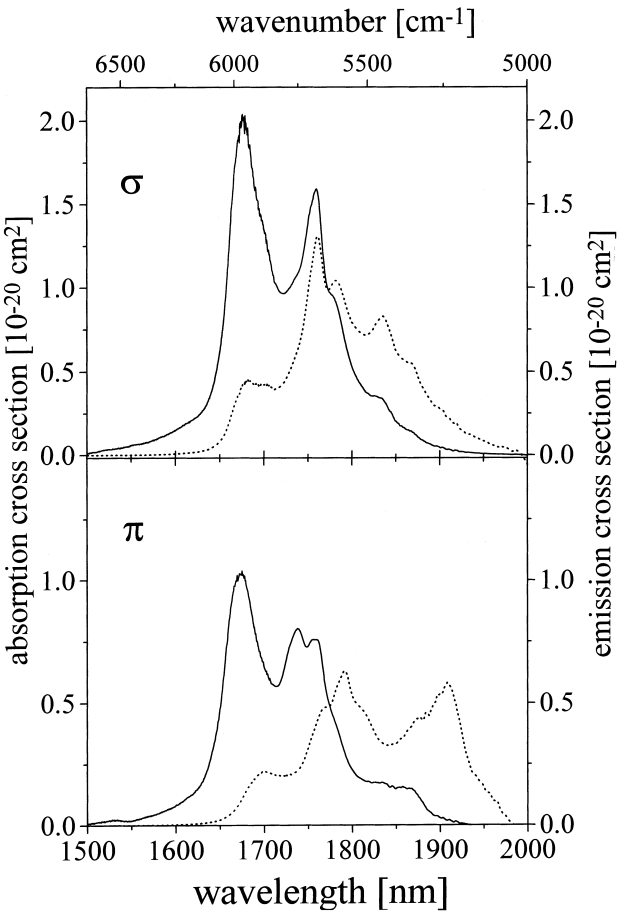

Fig. 4. The absorption cross section for the $^3H_6$–$^3F_4$ transition of Tm^{3+} in $LiTaO_3$ and derived the $^3F_4$–$^3H_6$ emission cross section.

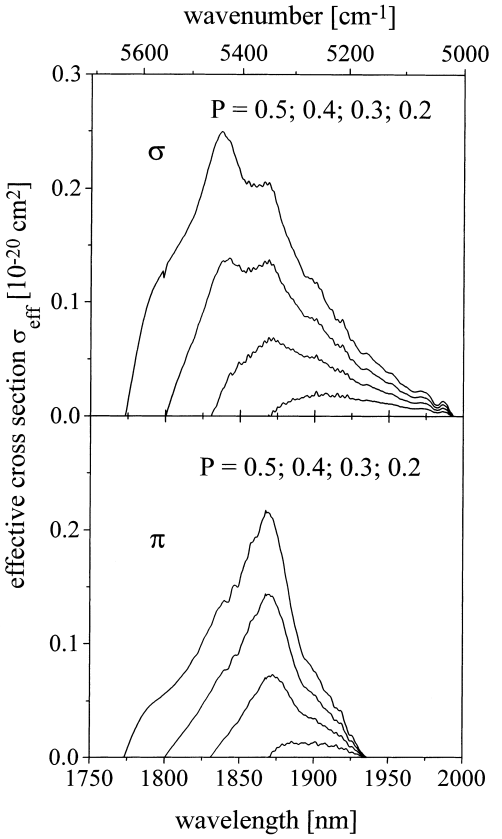

Fig. 5. The effective cross section for the $^3F_4$–$^3H_6$ transition of Tm^{3+} in $LiTaO_3$.

Results of calculation for several P parameters likely to be achieved in real laser systems are shown in Fig. 5. Both the emission cross section values and the predicted tunability range are promising.

Limiting step in the population build up on the $^3F_4$ level is relative long lifetime of the $^3H_4$ level amounting to 210 μs for $LiTaO_3$ crystal containing 9.5×10^{19} ions/cm^3. It has been shown that the $^3H_4$ excitation may be efficiently removed by a cross relaxation process in heavy doped Tm crystals, but it is not known yet whether such concentration may be attained in $LiTaO_3$ or $LiNbO_3$ crystals.

In Fig. 6 we present a partial energy level scheme for $LiTaO_3$:Ho. The calculated emission cross sections for the $^5I_7$–$^5I_8$ transition are shown in Figs. 7 and 8. Disadvantage of holmium doped crystals is related to pumping efficiency. The $^5I_8$–$^5I_4$ absorption band matches an emission band of AlGaAs laser diode, but the absorption intensity is extremely low. Efficient pumping via the $^5F_5$ level is possible, unfortunately the power of available red laser diodes is low.

4. Relaxation of excited states

Excited states decay by competitive radiative transitions, multiphonon relaxation and ion–ion processes. Relative contribution of these decay routes should be known at least

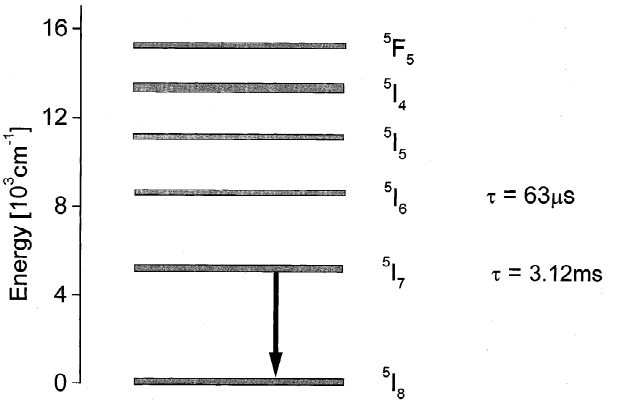

Fig. 6. The partial energy level scheme for Ho^{3+} in $LiTaO_3$.

for these laser schemes in which the upper laser level is not excited directly. Radiative transition rates can be evaluated conveniently by Judd–Ofelt treatment. Then multiphonon relaxation rates can be derived from radiative transition rates and measured lifetimes for activator concentration sufficiently low to neglect the ion–ion interaction. In Fig. 9 the multiphonon relaxation rates for Er in $LiNbO_3$ are plotted versus energy gap between luminescent level and next lower lying level. This linear depen-

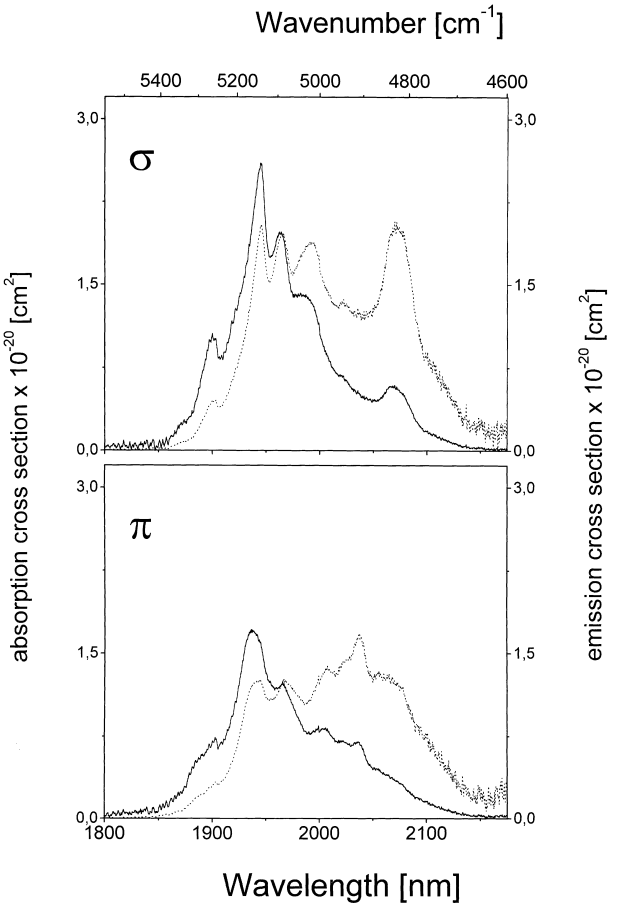

Fig. 7. The absorption cross section for the $^5I_8$–$^5I_7$ transition of Ho^{3+} in $LiTaO_3$ and derived the $^5I_7$–$^5I_8$ emission cross section.

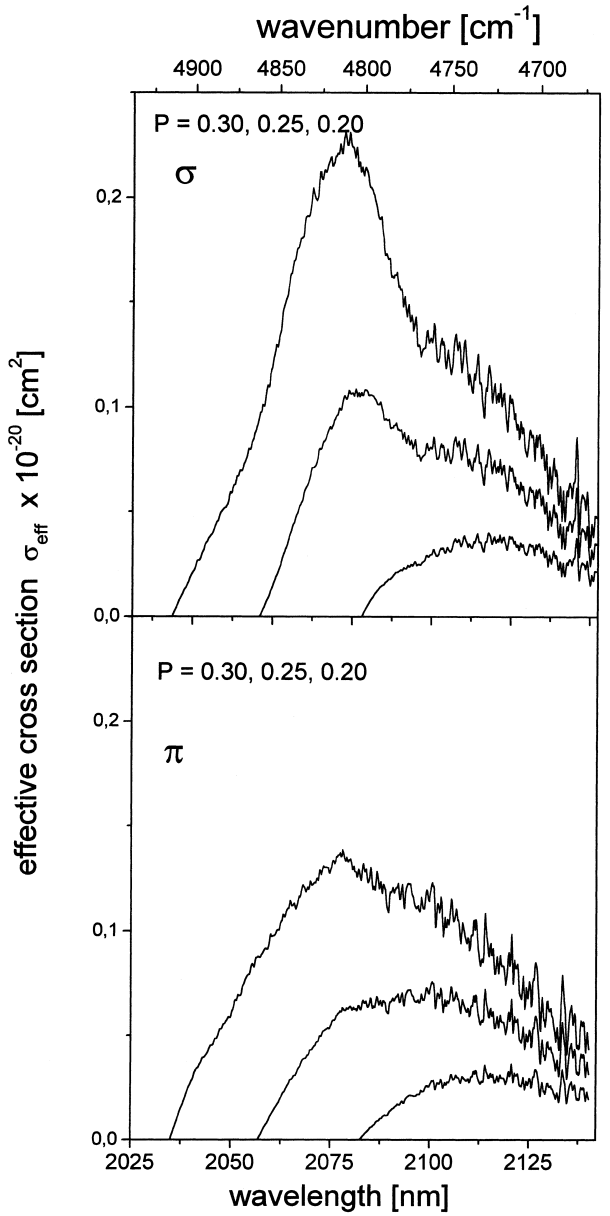

Fig. 8. The effective cross section for the transition $^5I_7$–$^5I_8$ of Ho^{3+} in $LiTaO_3$.

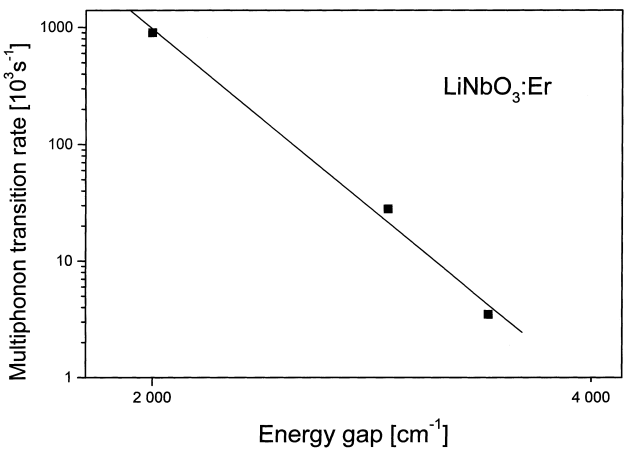

Fig. 9. The multiphonon transition rate for Er^{3+} in $LiNbO_3$ versus energy gap between luminescent level and next lower lying level.

Table 2
Calculated radiative lifetimes τ_{rad} and measured lifetimes τ_m of luminescent states of Tm in $LiTaO_3$ and $LiNbO_3$

Level	$LiTaO_3$:Tm			[c]$LiNbO_3$:Tm	
	τ_{rad} [μs]	τ_m [μs][a]	τ_m [μs][b]	τ_{rad} [μs]	$\tau_{m.}$ [μs]
$^1D_2$	29	8	4.6	10	6.1
$^1G_4$	274	95	38	205	103
$^3H_4$	456	210	110	342	240
$^3F_4$	953	2510	2380	1730	2700

[a] $C_{Tm}=9.5\times10^{19}$ ions/cm^3.
[b] $C_{Tm}=1.7\times10^{20}$ ions/cm^3.
[c] Taken from Ref. [15].

Table 3
Calculated radiative lifetimes τ_{rad} and measured lifetimes $\tau_{m.}$ of luminescent states of Ho in $LiTaO_3$ and $LiNbO_3$

Level	$LiTaO_3$:Ho		$LiNbO_3$:Ho[a]	
	τ_{rad} [μs]	τ_m [μs][a]	τ_{rad} [μs]	τ_m [μs]
$^5S_2$	57	13	109	9
$^5F_5$	56	0.5	79	9
$^5I_6$	676	63		
$^5I_7$	1766	3120		

[a] Taken from Ref. [16].

dence known as 'energy gap law' may be used to assess the multiphonon relaxation rates for other levels of ions. The radiative lifetimes and the measured lifetimes for luminescent levels of Tm and Ho in $LiTaO_3$ crystal are given in Tables 2 and 3. For a comparison the published data concerning $LiNbO_3$:Tm and $LiNbO_3$:Ho are shown in last columns of the tables. It can be seen that measured lifetimes are shorter than radiative lifetimes except for first excited states. Taking into account predictions of an energy gap law we conclude that the ion–ion interaction contribute to the decay through cross relaxation process. In addition to downward transition the upward transitions should be accounted for when exciting by powerful narrow band sources. Up-conversion of pumping light at wavelength ~0.8 μm and ~1 μm in $LiNbO_3$:Er is well documented [17,18]. In Fig. 10 we show the up-converted luminescence band excited in $LiTaO_3$:Ho by 647.1 nm line of Kr ion laser. This luminescence can not be excited by a short pulse pumping, therefore we suppose that the mechanism involved is an excited state absorption from the $^5I_7$ level.

5. Conclusions

Effective emission cross sections evaluated for $LiTaO_3$:Tm and $LiTaO_3$:Ho are promising, however further investigation is needed to elucidate and possibly improve the efficiency of excitation transfer from pump levels to upper laser levels. Data concerning relaxation of excited states in particular contribution of ion–ion interaction should be considered as preliminary.

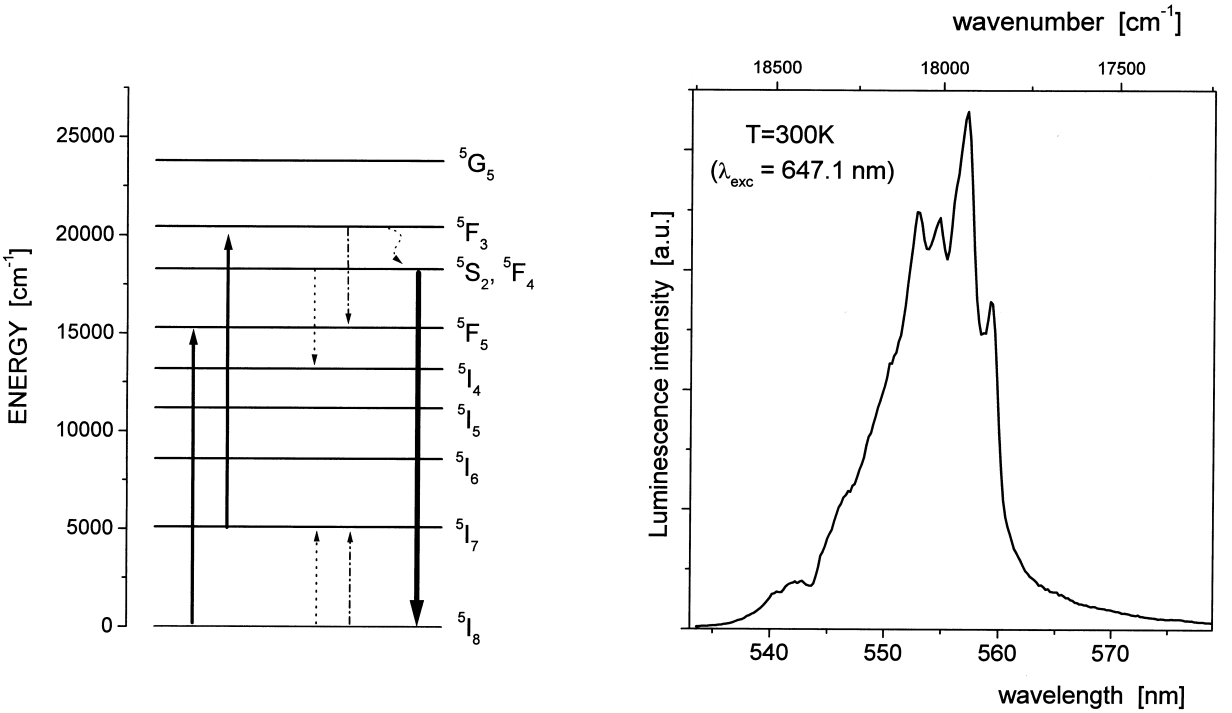

Fig. 10. The energy level scheme and the $^5S_2$–$^5I_8$ transition excited in $LiTaO_3$:Ho by 647.1 nm line of Kr ion laser.

References

[1] M.E. Lines, A.M. Glass, Principles and Applications of Ferroelectrics and Related Materials, Clarendon Press, Oxford, 1997.
[2] P. Gunter, J.P. Huignard (Eds.), Photorefractive Materials and Their Applications, Vols. I and II, Springer Verlag, Berlin, 1998.
[3] A.M. Prokhorov, Yu.S. Kuzminov, Ferroelectric Crystals For Laser Radiation Control, A. Hilger Publishing, Bristol, 1990.
[4] L.F. Johnson, A.A. Ballman, J. Appl. Phys. 40 (1969) 297.
[5] E. Lallier, J.P. Pocholle, M. Papuchon, C. Greezes-Besser, E. Pelletier, M. De Micheli, M.J. Li, Q. He, D.B. Ostrovsky, Electron. Lett. 25 (1989) 1491.
[6] N.A. Sauford, J.A. Aust, K.J. Malone, D.R. Larson, A. Roshko, Optics Lett. 17 (1992) 1578.
[7] E. Lallier, D. Papillon, J.P. Pocholle, M. Papuchon, M. De Micheli, D.B. Ostrovsky, Electron. Lett. 29 (2) (1993) 175.
[8] K.S. Abedin, M. Sato, H. Ito, T. Maeda, K. Shimamura, T. Fukuda, J. Appl. Phys. 78 (1995) 691.
[9] R. Brinkman, W. Sohler, H. Suche, Electron. Lett. 27 (1991) 415.
[10] J. Garcia-Sole, Phys. Script T55 (1994) 30.
[11] D.M. Gill, L. Mc Caughan, J.C. Wright, Phys. Rev. B 53 (1996) 2334.
[12] W. Ryba-Romanowski, S. Golab, W.A. Pisarski, G. Dominiak-Dzik, M.N. Palatnikov, N.V. Sidorov, V.T. Kalinnikov, Appl. Phys Lett. 70 (1997) 19.
[13] J. Garcia-Sole, A. Lorenzo, T. Petit, G. Boulon, B. Roux, H. Jaffrezic, Journal de Physique IV 4 (1994) C293.
[14] R. Burlot, R. Moncorge, H. Manaa, G. Boulon, Y. Guyot, J. Garcia-Sole, D. Cochet-Muchy, Optical Mater. 6 (1996) 313.
[15] L. Nunez, J.O. Tocho, J.A. Sanz-Garcia, E. Rodriguez, F. Cusso, D.C. Hanna, A.C. Tropper, A.C. Large, J. Luminescence 55 (1993) 253.
[16] A. Lorenzo, L.E. Bausa, J.A. Sanz Garcia, J. Garcia Sole, J. Phys. Condens. Matter. 8 (1996) 5781.
[17] J. Zheng, Y. Lu, G. Luo, J. Ma, Y. Lu, Appl. Phys. Lett. 72 (1998) 1808.
[18] L. Nunez, B. Herreros, R. Duchowicz, G. Lifante, J.O. Tocho, F. Cusso, J. Luminescence 60–61 (1994) 81.